Monthly Notices of the Royal Astronomical Society

MNRAS **436,** 89–100 (2013)
Advance Access publication 2013 September 25

doi:10.1093/mnras/stt1517

Testing gravity using large-scale redshift-space distortions

Alvise Raccanelli,[1,2★] Daniele Bertacca,[3,4] Davide Pietrobon,[1] Fabian Schmidt,[2] Lado Samushia,[5] Nicola Bartolo,[4,6] Olivier Doré,[1,2] Sabino Matarrese[4,6] and Will J. Percival[5]

[1] *Jet Propulsion Laboratory, California Institute of Technology, Pasadena, CA 91109, USA*
[2] *California Institute of Technology, Pasadena, CA 91125, USA*
[3] *Physics Department, University of the Western Cape, Cape Town 7535, South Africa*
[4] *Dipartimento di Fisica e Astronomia 'G. Galilei', Università degli Studi di Padova, via F. Marzolo 8, I-35131 Padova, Italy*
[5] *Institute of Cosmology and Gravitation, University of Portsmouth, Dennis Sciama Building, Portsmouth P01 3FX, UK*
[6] *INFN Sezione di Padova, via F. Marzolo 8, I-35131 Padova, Italy*

Accepted 2013 August 11. Received 2013 August 11; in original form 2012 July 13

ABSTRACT

We use luminous red galaxies from the Sloan Digital Sky Survey (SDSS) II to test the cosmological structure growth in two alternatives to the standard Λ cold dark matter (ΛCDM)+general relativity (GR) cosmological model. We compare observed three-dimensional clustering in SDSS Data Release 7 (DR7) with theoretical predictions for the standard vanilla ΛCDM+GR model, unified dark matter (UDM) cosmologies and the normal branch Dvali–Gabadadze–Porrati (nDGP). In computing the expected correlations in UDM cosmologies, we derive a parametrized formula for the growth factor in these models. For our analysis we apply the methodology tested in Raccanelli et al. and use the measurements of Samushia et al. that account for survey geometry, non-linear and wide-angle effects and the distribution of pair orientation. We show that the estimate of the growth rate is potentially degenerate with wide-angle effects, meaning that extremely accurate measurements of the growth rate on large scales will need to take such effects into account. We use measurements of the zeroth and second-order moments of the correlation function from SDSS DR7 data and the Large Suite of Dark Matter Simulations (LasDamas), and perform a likelihood analysis to constrain the parameters of the models. Using information on the clustering up to $r_{\rm max} = 120\,h^{-1}$ Mpc, and after marginalizing over the bias, we find, for UDM models, a speed of sound $c_\infty \leq 6.1\text{e-}4$, and, for the nDGP model, a cross-over scale $r_{\rm c} \geq 340$ Mpc, at 95 per cent confidence level.

Key words: methods: analytical – cosmological parameters – cosmology: observations – large-scale structure of Universe.

1 INTRODUCTION

The strangest feature of our current cosmological model is the observation that the expansion rate of the Universe is accelerating (Riess et al. 1998; Perlmutter et al. 1999). Understanding the cause of cosmic acceleration is one of the great challenges of physics. It has been speculated that the cause of this acceleration is a cosmological constant, or perhaps some novel form of matter; our ignorance is summarized by the simple name for the cause of the observed phenomenon: 'dark energy'. Alternatively, it could be explained by the breakdown of Einstein's general relativity (GR) theory of gravitation on cosmological scales (see Durrer & Maartens 2008 for a review on different dark energy and modified gravity models). Observations of the large-scale structure of the Universe have played an important role in developing our standard cosmological model and will play an essential role in our investigations of the origin of cosmic acceleration.

We will illustrate how it is possible to test GR and alternative models of gravity using luminous red galaxies (LRGs) from the Sloan Digital Sky Survey (SDSS) Data Release 7 (DR7) data. To estimate the statistical errors on our measurements we use galaxy catalogues from the Large Suite of Dark Matter Simulations (LasDamas; McBride et al., in preparation)[1] that are designed to model the clustering of SDSS galaxies.

★ E-mail: raccanelli@gmail.com

[1] http://lss.phy.vanderbilt.edu/lasdamas/

The presence of a dark energy component in the energy density of the Universe (or the fact that our theory of gravity needs to be modified on large scales) modifies the gravitational growth of large-scale structures. The large-scale structure we see traced by the distribution of galaxies arises through gravitational instability, which amplifies primordial fluctuations that originated in the very early Universe; the rate at which structure grows from small perturbations offers a key discriminant between cosmological models, as different models predict measurable differences in the growth rate of large-scale structure with cosmic time (e.g. Jain & Zhang 2007; Song & Koyama 2009; Song & Percival 2009). For instance, dark energy models in which general relativity is unmodified predict different large-scale structure formation compared to modified gravity models with the same background expansion (e.g. Dvali, Gabadadze & Porrati 2000; Carroll et al. 2004; Brans 2005; Nesseris & Perivolaropoulos 2008; Yamamoto, Sato & Hütsi 2008; Yamamoto et al. 2010).

Observations of redshift-space distortions (RSD) in spectroscopic galaxy surveys are a promising way to study the pattern and the evolution of the large-scale structure of the Universe (Kaiser 1987; Hamilton 1998), as they provide constraints on the amplitude of peculiar velocities induced by structure growth, thereby allowing tests of the theory of gravity governing the growth of those perturbations. RSD have been measured using techniques based on both correlation functions and power spectra (Peacock et al. 2001; Hawkins et al. 2003; Pope et al. 2004; Zehavi et al. 2005; Tegmark et al. 2006; Guzzo et al. 2008; Okumura et al. 2008; Percival & Schäfer 2008; Cabré & Gaztañaga 2009; Blake et al. 2011); the most recent analyses come from the Baryon Oscillation Spectroscopic Survey (BOSS) Data Release 9 (DR9) catalogue (Reid et al. 2012; Sanchez et al. 2012).

A key element of RSD is that the motion of galaxies is independent of their properties and of the bias, that relates the baryonic matter to the total mass; therefore, measurements of peculiar velocity directly probe the matter distribution. They also are complementary to other probes, since they depend on temporal metric perturbations, while e.g. weak lensing depends on the sum of the temporal and spatial metric perturbations and the integrated Sachs–Wolfe (ISW) effect depends on the sum of their derivatives.

The standard analysis of RSD makes use of the so-called Kaiser formalism that relies on some assumptions, including considering only the linear regime and the distant observer approximation, and restrains the range of usable scales to 30–60 h^{-1} Mpc. There have been several attempts to model smaller scales RSD, exploring the quasi-linear regime (e.g. Scoccimarro 2004; Taruya, Nishimichi & Saito 2010; Reid & White 2011; Kwan, Lewis & Linder 2012); recently Bertacca et al. (2012) developed a formalism to compute the correlation function including GR corrections that arise when probing scales comparable to the Hubble scales.

In this paper we show how precise measurements of the clustering of galaxies can be used to test cosmological models; we make use of the wide-angle methodology as tested in Raccanelli, Samushia & Percival (2010), that drops the distant observer approximation, combined with prescriptions and measurements of SDSS-II data from Samushia, Percival & Raccanelli (2012), to constrain two interesting alternatives to the standard cosmology: a particular class of unified dark matter (UDM) models (Bertacca et al. 2008; Bertacca, Bartolo & Matarrese 2010) and the normal branch Dvali–Gabadadze–Porrati (DGP; Schmidt 2009). In the process, we also derive a parametrized formula for the growth factor in UDM models, and we show that wide-angle corrections are degenerate with variations of the rate of the growth of structures, demonstrating the need to include them if one wants to measure the growth rate at per cent level.

The paper is organized as follows: in Section 2 we briefly review the theory of RSD; in Section 3 we present the catalogue used; the methodology used to perform measurements is reviewed in Appendix A; in Section 4 we introduce the parametrization of structure growth we apply in our tests and discuss degeneracies that arise from a more comprehensive description of the data; after discussing the theoretical growth of structures for the non-standard cosmological models, we present the measurements in Section 5, and set limits on the parameters in Section 6; finally, in Section 7, we conclude and discuss our results.

2 REDSHIFT-SPACE DISTORTIONS

RSD arise because we infer galaxy distances from their redshifts using the Hubble law: the radial component of the peculiar velocity of individual galaxies will contribute to each redshift and will be misinterpreted as being cosmological in origin, thus altering our estimate of the distances to them. The relation between the redshift-space position $\boldsymbol{s}$ and real-space position $\boldsymbol{r}$ is

$$\boldsymbol{s}(\boldsymbol{r}) = \boldsymbol{r} + v_r(\boldsymbol{r})\hat{\boldsymbol{r}}, \tag{1}$$

where v_r is the velocity in the radial direction.

The measured clustering of galaxies will therefore be anisotropic and the additional radial signal can be used to determine the characteristic amplitude of the pair-wise distribution of the peculiar velocities at a given scale, which in turn depends on the growth rate.

Measurements are normally obtained over a small range of scales, because of simplified modelling. In this work, we use the extended analysis tested in Raccanelli et al. (2010) and Samushia et al. (2012), which includes a more realistic description of the geometry of the system, dropping the plane-parallel approximation; this allows us to fit the observed galaxy correlation function on a larger range of scales, and therefore to be more sensitive to the cosmological parameter variations.

By imposing the conservation of the number of galaxies we can derive the Jacobian for the real- to redshift-space transformation (at the linear order):

$$\delta^s(\boldsymbol{s}) = \delta^r(\boldsymbol{r}) - \left(\frac{\partial v}{\partial r} + \frac{\alpha(\boldsymbol{r})v}{r}\right), \tag{2}$$

where $\delta^{s,\,r}$ are the observed redshift- and real-space galaxy overdensity at positions s and r, and

$$\alpha(\boldsymbol{r}) = \frac{\partial \ln r^2 \bar{N}^r(\boldsymbol{r})}{\partial \ln r}, \tag{3}$$

and $\bar{N}^r(\boldsymbol{r})$ is the expected galaxy distribution in real space. The simplest statistic that can be constructed from the overdensity field is the correlation function $\xi(r_{12})$, defined as

$$\xi(r_{12}) \equiv \langle \delta(\boldsymbol{r}_1)\,\delta(\boldsymbol{r}_2)\rangle. \tag{4}$$

In linear theory, all of the information is enclosed in the first three even coefficients of the Legendre polynomial expansion of the function ξ (Hamilton 1992):

$$\xi(r, \mu) = \xi_0(r)L_0(\mu) + \xi_2(r)L_2(\mu) + \xi_4(r)L_4(\mu), \tag{5}$$

where L_ℓ are the Legendre polynomials and μ is the cosine of the angle with the line of sight ($\mu = \cos(\phi)$ in Fig. A1).

In this work we will use measurements of the moments of the correlation function from the SDSS DR7 catalogue, using a methodology that takes care of several corrections, as we will describe in the next sections.

3 THE SLOAN DIGITAL SKY SURVEY

We use data from the SDSS-II DR7, which obtained wide-field CCD photometry (Gunn et al. 1998) in five passbands (u, g, r, i, z; e.g. Fukugita et al. 1996), amassing nearly 10 000 deg^2 of imaging data for which the object detection is reliable down to $r \sim 22$ (Abazajian et al. 2009). From these photometric data, LRGs were targeted (Eisenstein et al. 2001) and spectroscopically observed, yielding a sample of 106 341 LRGs in the redshift bin $0.16 < z < 0.44$.

An estimate of the statistical errors associated with the measurements is achieved through LasDamas mock catalogues, which model the clustering of SDSS galaxies in the redshift span $0.16 < z < 0.44$. The simulations are produced by placing artificial galaxies inside dark matter haloes using a halo occupation distribution (HOD) with parameters measured from the SDSS galaxy sample. We use the 80 ‘Oriana’ catalogues that have exactly the same angular mask as the SDSS survey and subsample them to match the redshift distribution of the LRGs in our SDSS DR7 data set. Further details regarding the angular and redshift distribution of galaxies in random catalogues can be found in Samushia et al. (2012).

3.1 Methodology

To perform our analysis of cosmological models we use the methodology presented in Raccanelli et al. (2010) and measurements of SDSS-II data from Samushia et al. (2012). In Appendix A we briefly revisit the main aspects of the approach we followed; this drops the distant observer approximation and includes a careful treatment of survey geometry, non-linear effects and the distribution of pair orientation. This allows us to consider a wide range of scales (we use measurements from 30 to 120 h^{-1} Mpc).

4 PARAMETRIZING THE GROWTH OF STRUCTURE

Measuring the matter velocity field at the locations of the galaxies gives an unbiased measurement of $f\sigma_{8\mathrm{m}}$, provided that the distribution of galaxies randomly samples matter velocities, where

$$f = \frac{\mathrm{d}\ln D}{\mathrm{d}\ln a} \tag{6}$$

is the logarithmic derivative of the linear growth rate, $D(a) \propto \delta_\mathrm{m}$, with respect to the scale factor a (δ_m being the fractional matter density perturbation) and $\sigma_{8\mathrm{m}}$ quantifies the amplitude of fluctuations in the matter density field.

Linder (2005) proposed a gravitational growth rate formalism, which parametrizes the growth factor as

$$D(a) = a\,\exp\left[\int_0^a \left[\Omega_\mathrm{m}^\gamma(a') - 1\right]\frac{\mathrm{d}a'}{a'}\right], \tag{7}$$

which leads to the following expression for f:

$$f = [\Omega_\mathrm{m}(a)]^\gamma\,, \tag{8}$$

with

$$\Omega_\mathrm{m}(a) = \frac{\Omega_\mathrm{m} a^{-3}}{\sum_i \Omega_i\,\exp\left[3\int_a^1 [w_i(a') + 1]\,\frac{\mathrm{d}a'}{a'}\right]}, \tag{9}$$

where the summation index goes over all the components of the Universe (i.e. dark matter, dark energy, curvature, radiation). Within this formalism, γ is a parameter that is different for different cosmological models: in the standard ΛCDM+GR model it is constant, $\gamma \approx 0.55$, while it is $\approx$0.68 for the self-accelerating DGP model (see e.g. Linder 2005). In some other cases, it is a function of the cosmological parameters or redshift, as we will discuss. It should be noted, however, that the parametrization given by equation (7) does not necessarily describe the growth rate in non-standard cosmologies.

Given that, as we will see, ξ_ℓ depend on f, measuring RSD allows us to determine γ, and hence to test different cosmological models. This also provides a good discriminant between modified gravity and dark energy models, as argued by Linder (2005, 2007) and Guzzo et al. (2008).

4.1 Degeneracy $\theta - \gamma$

In Appendix A we review the methodology used to obtain measurements of multipoles of the correlation function; our methodology involves corrections with respect to standard analyses, and in particular it drops the distant observer approximation ($\theta = 0$ in Fig. A1). The error in the estimate of the correlation function induced by assuming $\theta = 0$ can lead to a wrong estimate of the cosmological parameters measured with RSD.

We show this in Fig. 1, where is plotted, for different redshifts, the error in estimating γ when neglecting the wide-angle corrections (in the case of $\phi = \pi/2$, see Fig. A1), as a function of θ. The wide-angle corrections will be more important for surveys probing low redshifts, as the same scale is seen over a larger angular separation. However, the redshift dependence of the corrections is non-trivial (see Papai & Szapudi 2008 for their expressions). A detailed comparison of the plane-parallel to the wide-angle case is not straightforward, as the linear distance of the pair depends on the redshift and the angular separation; when integrating over μ of equation (A11), assuming $\theta = 0$ and keeping the same z would be a non-physical case. The plot in Fig. 1 is just one example to show that neglecting θ is degenerate with varying γ. The overall importance of the corrections will depend on the relative distributions of

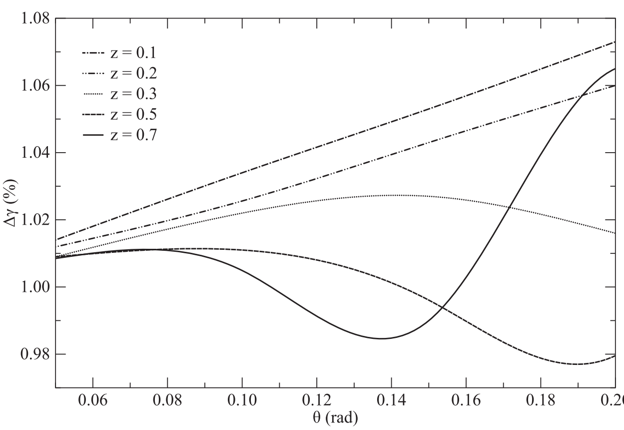

Figure 1. Percentage error in the measurement of γ when neglecting the wide-angle corrections, for $\phi = \pi/2$, as a function of θ, at different redshifts.

θ within the specific survey (i.e. Fig. A2 for the SDSS-II DR7 data used in this paper).

A more careful analysis of the influence of wide-angle and other large-scale corrections for future *Euclid*-like and Square Kilometre Array (SKA)-like surveys is left to a future work.

5 MEASUREMENTS

The moments of the correlation function are sensitive to the γ parameter through the function *f*. In this work we concentrate on two alternatives to the standard ΛCDM+GR scenario: (i) the UDM cosmology (Bertacca et al. 2008, 2010), and (ii) the normal branch DGP model including Dark Energy (nDGP) of Schmidt (2009). These two models deviate from the standard cosmology in different ways: the UDM model assumes a single dark fluid with a clustering part, and leaves GR unmodified, while in nDGP, gravity crosses over from 4D to 5D above a cross-over scale r_c (see Sections 5.1 and 5.2 for details). For the UDM model, we use the values of γ of equation (15) for a set of values of the speed of sound c_∞, while for nDGP we compute the growth solving explicitly equation (17).

As one can see in equation (A4), the wide-angle and mode-coupling corrections are described by a set of terms that depend on $\{r, \theta, \phi, \gamma\}$, and this means that wide-angle corrections are also different for different models of gravity. In Figs 2 and 3 we show the wide-angle corrections to the monopole and quadrupole of the correlation function for the different models, compared to the ΛCDM+GR case.

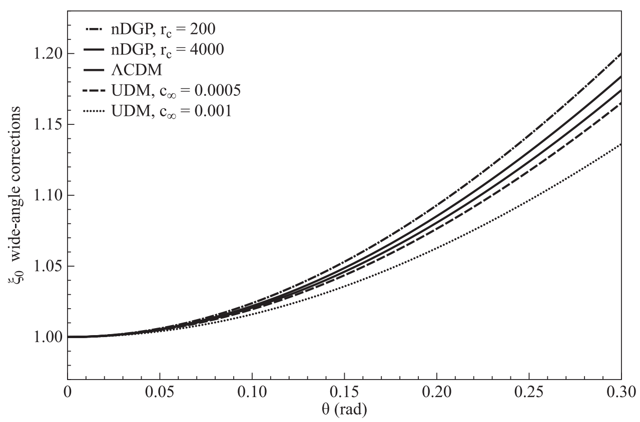

Figure 2. Wide-angle corrections (i.e. $\xi_0(r, \theta)/\xi_0(r, \theta = 0)$) to the monopole of the correlation function for the models considered and different values of their parameter.

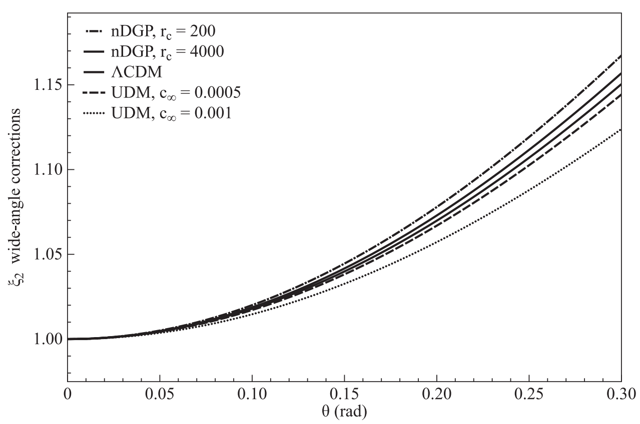

Figure 3. Wide-angle corrections (i.e. $\xi_2(r, \theta)/\xi_2(r, \theta = 0)$) to the quadrupole of the correlation function for the models considered and different values of their parameter.

5.1 UDM

Assuming a flat Friedmann–Lemaître–Robertson–Walker (FLRW) background metric with scale factor $a(t)$, Bertacca et al. (2008, 2010) introduced a class of UDM scalar field models which, by allowing a pressure equal to $-c^2\rho_\Lambda$ on cosmological scales, reproduces the same background expansion as the ΛCDM one. In such a way, a single scalar field can be responsible for both the late time accelerated expansion for the Universe and of the growth of structure. When the energy density of radiation becomes negligible, the background evolution of the Universe is completely described by

$$H^2(z) = H_0^2\left[\Omega_{\Lambda 0} + \Omega_{\rm m0}(1+z)^3\right], \tag{10}$$

where H is the Hubble parameter, $H_0 = H(z=0)$ and z is the redshift. $\Omega_{\Lambda 0}$ and $\Omega_{\rm m0} = 1 - \Omega_{\Lambda 0}$ can be interpreted as the 'cosmological constant' and 'dark matter' density parameters, respectively.

The density contrast of the clustering component is $\delta_{\rm DM} \equiv \delta\rho/\rho_{\rm DM}$, where $\rho_{\rm DM} = \rho - \rho_\Lambda$ is the only component of the scalar field density that clusters. In these models one of the most relevant parameters is the sound speed of the perturbations, which defines a typical sound-horizon (Jeans length) scale above which growth of structure is possible (Bertacca & Bartolo 2007). Following Bertacca et al. (2011), for scales smaller than the cosmological horizon and $z < z_{\rm rec}$, we have that

$$\delta_{\rm DM}\left[k;\eta(z)\right] = T_{\rm UDM}\left[k;\eta(z)\right]\delta_{\rm m}\left[k;\eta(z)\right], \tag{11}$$

where $\delta_{\rm m}$ is the matter density perturbation in the standard ΛCDM model, η is the conformal time and $T_{\rm UDM}(k;\eta)$ is the transfer function for the UDM model:

$$T_{\rm UDM}(k;\eta) = j_0[\mathcal{A}(\eta)k], \tag{12}$$

$$\mathcal{A}(\eta) = \int^{\eta} c_{\rm s}(\eta')\,{\rm d}\eta', \tag{13}$$

$$c_{\rm s}^2(a) = \frac{\Omega_{\Lambda 0}c_\infty^2}{\Omega_{\Lambda 0} + (1-c_\infty^2)\Omega_{\rm m0}a^{-3}}. \tag{14}$$

We then define the parameter c_∞ as the value of the sound speed when $a \to \infty$.

In this model, the growth factor is computed correcting the ΛCDM one with the transfer function of equation (12); its deviation from the standard model case, as a function of c_∞ for different values of k, is plotted in Fig. 4. The effect of the baryons is included implicitly in the definition of $\delta_{\rm m}$, where we have used the matter transfer function $T_{\rm m}$ suggested in Eisenstein & Hu (1998); for more details see section 2.1.2 of Bertacca et al. (2010).

We refer to Bertacca et al. (2008, 2010, 2011) for details of the UDM models considered (see also Camera et al. 2009, 2010; Piattella & Bertacca 2011; Camera, Carbone & Moscardini 2012).

Using the transfer function of equation (12), one can obtain a new result, which is particularly relevant for the present analysis: the parametrization of the growth rate in UDM models, which turns out to be

$$\gamma_{\rm UDM}(a,k,c_\infty) = \frac{\ln\left[\frac{{\rm d}\ln T_{\rm UDM}(a,k,c_\infty)}{{\rm d}\ln a} + f_{\Lambda{\rm CDM}}(a)\right]}{\ln\Omega_{\rm m}(a)}; \tag{15}$$

as one can see, $\gamma_{\rm UDM}$ depends on (a, k, c_∞), and in Fig. 5 is shown its value as a function of them.

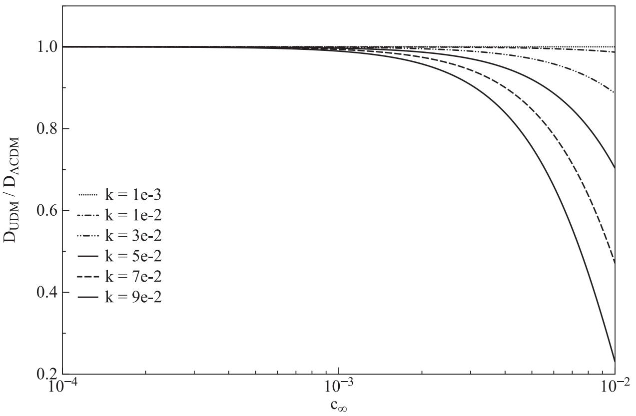

Figure 4. Deviation of the growth factor for the UDM model, as a function of the speed of sound c_∞, for different values of k.

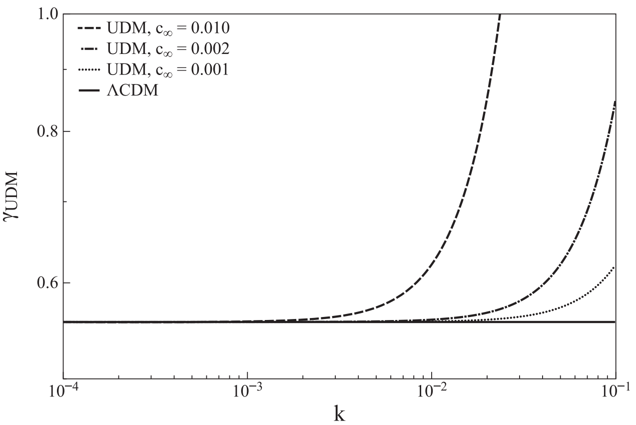

Figure 5. $\gamma_{\rm UDM}$ as a function of k, for different values of c_∞ (at $z = 0.15$), compared with the ΛCDM+GR case.

Equation (15) gives the value of γ for UDM cosmologies; it depends on redshift, scale and speed of sound. Fig. 5 shows that $\gamma_{\rm UDM} \geq \gamma_{\Lambda\rm CDM}$. Actually this is easy to understand: one of the features of the UDM models is that, under the Jeans length, the density contrast decreases while oscillating in time (see e.g. Bertacca & Bartolo 2007; Bertacca et al. 2011). This means that, compared to the ΛCDM model, there is a further suppression in the growth of structures. Notice also that there are some values of c_∞ that give non-physical results when one uses the parametrization of equation (15); however, even using equation (6), the growth rate for these values becomes highly oscillatory, so we will consider them ruled out. For this reason, given that we will limit our analysis to linear scales, and accounting also for existing limits on UDM models (e.g. Bertacca et al. 2011) we will consider values of $c_\infty \lesssim 0.002$.

In Figs 6 and 7 we show the comparison of measurements of the zeroth and second-order moments of the correlation function measured from SDSS DR7 with the theoretical predictions for UDM models, for several values of the speed of sound parameter c_∞.

5.2 DGP

In the DGP (Dvali et al. 2000) model, all matter and radiation are confined to a four-dimensional brane in five-dimensional Minkowski space. Gravity, while restricted to the brane on small scales, propagates into the extra dimension above the cross-over

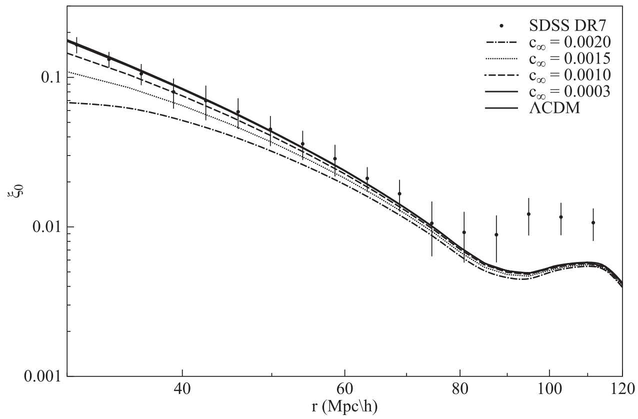

Figure 6. ξ_0 measured from SDSS DR7 and theoretical predictions for ΛCDM and UDM with different values of the speed of sound.

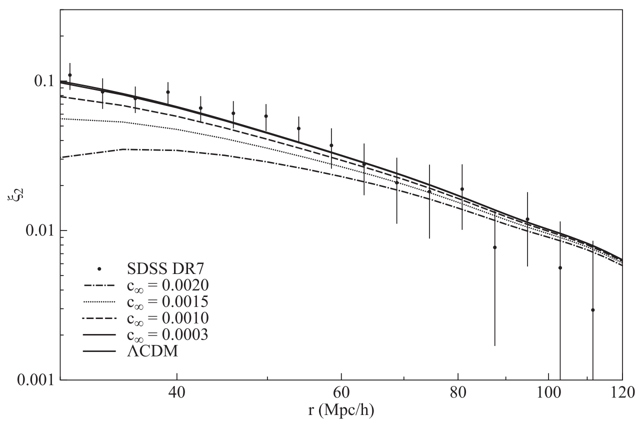

Figure 7. ξ_2 measured from SDSS DR7 and theoretical predictions for ΛCDM and UDM with different values of the speed of sound.

scale $r_{\rm c}$. This scenario admits an Friedmann–Robertson–Walker (FRW) cosmology on the brane (Deffayet 2001), where the Friedmann equation is modified to

$$H^2 \pm \frac{H}{r_{\rm c}} = \frac{8\pi G}{3} \left[\bar{\rho}_{\rm m} + \rho_{\rm DE}\right]. \quad (16)$$

The sign on the left-hand side depends on the choice of embedding of the brane. The negative sign (*accelerating branch*) leads to an accelerated expansion of the Universe at late times without a cosmological constant or dark energy (Deffayet 2001), i.e. $\rho_{\rm DE} = 0$ and $r_{\rm c} \sim H_0^{-1}$, while the positive sign (*normal branch*) does not yield acceleration by itself. The simplest self-accelerating model is in conflict with observations of the cosmic microwave background (CMB) and supernovae (e.g. Lombriser et al. 2009), and also has theoretical issues (Luty, Porrati & Rattazzi 2003; Nicolis & Rattazzi 2004; Gregory et al. 2007).

Here we consider a normal branch DGP model including a dark energy component $\rho_{\rm DE}$ to yield an accelerated expansion. Specifically, we use the model of Schmidt (2009) where the equation of state of the dark energy is tailored to yield an expansion history identical to ΛCDM for all $r_{\rm c}$. This model is not ruled out by expansion history probes or theoretical issues. Furthermore, it can serve as a toy model for more recent scenarios (deRham et al. 2008; Afshordi, Geshnizjani & Khoury 2009).

On scales much smaller than the horizon and smaller than $r_{\rm c}$, but yet large enough so that linear perturbation theory applies, the

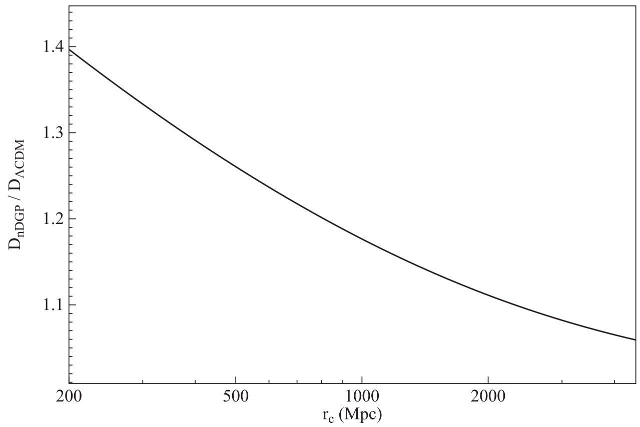

Figure 8. Deviation of the growth factor for the nDGP model, as a function of the cross-over scale r_c (see text for details).

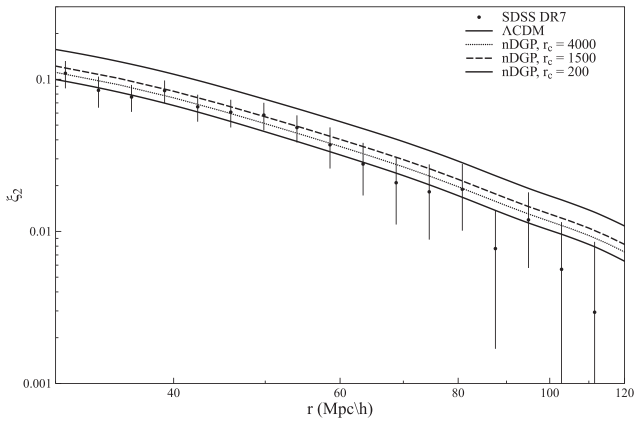

Figure 10. ξ_2 measured from SDSS DR7 and theoretical predictions for ΛCDM and nDGP, for some values of the cross-over scale r_c.

growth of perturbations during matter domination in these models is governed by (Koyama & Maartens 2006)

$$\ddot{\delta} + 2H\dot{\delta} = \frac{3}{2}\Omega_m(a)a^2H^2\left(1 + \frac{1}{3\beta(a)}\right)\delta, \quad (17)$$

where dots denote derivatives with respect to time, and

$$\beta = 1 \pm 2Hr_c\left(1 + \frac{aH'}{3H}\right). \quad (18)$$

Here the positive (negative) sign holds for the normal (self-accelerating) branch. Note that in the latter case, $\beta < 0$ and hence $G_{\rm eff} < G$, i.e. the growth of structure is slowed down with respect to GR. The opposite is the case for the normal branch ($\beta > 0$). In the case of the self-accelerating (sDGP) model with $\rho_{\rm DE} = 0$, Linder (2005) showed that the growth rate can be well described by the parametrization $f_{\rm sDGP}(a) = \Omega_m(a)^{\gamma_{\rm sDGP}}$, with $\gamma_{\rm sDGP} = 0.68$. For the normal branch model with dark energy (nDGP), this parametrization does not provide a good fit, and we use a numerical integration of equation (17) to derive the growth rate. The change in the growth with respect to ΛCDM is shown in Fig. 8 as a function of r_c.

In Figs 9 and 10 we show the comparison of the zeroth- and second-order moments of the correlation function measured from SDSS DR7 with the theoretical prediction for the nDGP model, for some values of the cross-over scale r_c.

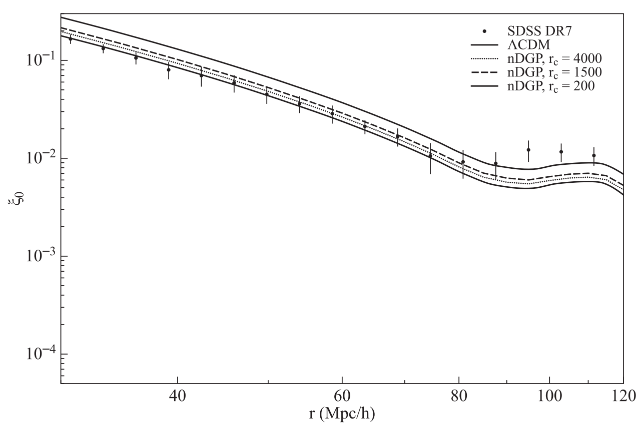

Figure 9. ξ_0 measured from SDSS DR7 and theoretical predictions for ΛCDM and nDGP, for some values of the cross-over scale r_c.

6 RESULTS

We compute the likelihood of the c_∞ and $1/r_c$ parameter for UDM and nDGP model, respectively, conditioned to the other parameters fixed to the *Wilkinson Microwave Anisotropy Probe* (*WMAP*) 7-year best-fitting ΛCDM model ones. We assume a Gaussian likelihood with covariance matrix described by equation (A10). This choice has the advantage of having the ΛCDM model as an asymptotic limit, when the extra parameter tends to zero.

We evaluated a joint $\mathcal{L}$ for the zeroth and second moments of the correlation function, focusing on two cases: (i) $r_{\rm max} = 80\,h^{-1}$ Mpc, where the data start to deviate from the mock for both ξ_0 and ξ_2 (see Figs A4 and A5), and (ii) $r_{\rm max} = 120\,h^{-1}$ Mpc, in order to investigate larger scales and where the data are still in reasonable agreement with the mocks. For larger scales, Ross et al. (2011) suggested (when considering a different sample) that the excess power can be due to systematic errors, so, to be conservative, we will not fit these scales.

The bias is poorly understood: in order to take into account its theoretical uncertainty, we leave it as a free parameter and marginalize over it. Since additional information on the bias can be independently inferred from other probes, as for example lensing measurements, we also derive the constraints on cosmological parameters which can be obtained when fixing the bias at its best-fitting value assuming a ΛCDM cosmology.

In Figs 11 and 12 we show the likelihood, as a function of c_∞(UDM) and $1/r_c$ (nDGP), in the $r_{\rm max} = 120\,h^{-1}$ Mpc case, assuming the knowledge of the bias (solid lines), and after marginalizing over it (dashed lines).

In Table 1 we report the best fit and the constraints on c_∞ and r_c at different confidence levels, for the various cases considered.

The bias plays a very important role: this was expected, since the shape of the correlation function is a weak function of the additional parameter in both classes of models, whereas the amplitude variation is large (in UDM the shape variation is more relevant, and increasingly important for larger values of c_∞).

In the UDM case, assuming the knowledge of the bias results in a best-fitting value of $c_\infty = 0$, which corresponds to the ΛCDM model, while, after marginalizing over the bias, the best fit is $c_\infty = 5 \times 10^{-4}$. From the Table 1 emerges that the constraints on the parameters are not sensitive to the maximum value of the distance between galaxy pairs. This is not surprising, as the deviation of the model from ΛCDM is larger for smaller scales (this can also be seen from Figs 6 and 7). It is interesting to note that, after

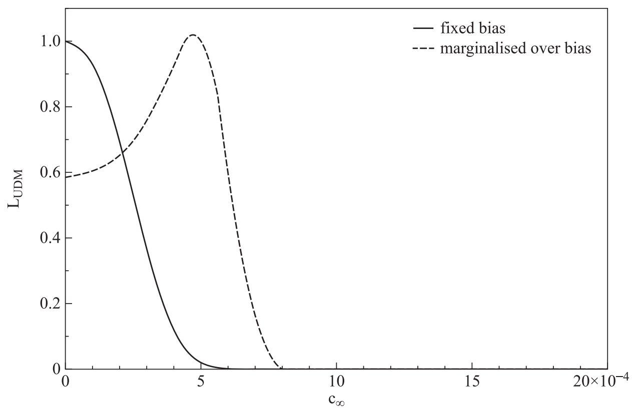

Figure 11. Likelihood for the UDM model, as function of the speed of sound c_∞, when assuming knowledge of the bias (solid line), and after marginalizing over it (dashed line).

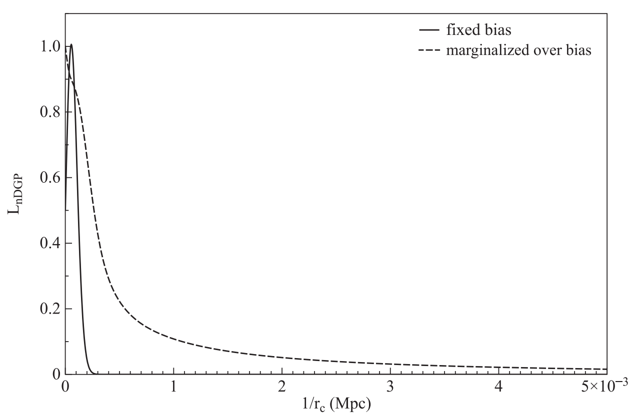

Figure 12. Likelihood for the nDGP model, as function of the inverse of the cross-over scale $1/r_c$, when assuming knowledge of the bias (solid line), and after marginalizing over it (dashed line).

bias marginalization, the best fit does not correspond to ΛCDM, meaning that the shape of the measured correlation functions is not fitted by ΛCDM; it would be interesting to perform a future analysis at different redshift or with other data sets (e.g. BOSS), to see how the peak of the likelihood will be modified. Our final constraint at 95 per cent confidence level, after marginalizing over the bias, is $c_\infty \leq 6.1 \times 10^{-4}$, almost two orders of magnitude better than previous constraints (Bertacca et al. 2011).

When considering the nDGP scenario, the effect of marginalizing over the bias is even more dramatic: the constraints on r_c worsen by a factor of ~20 (see Fig. 12 and Table 1). This occurs because the deviation from ΛCDM+GR of this model is scale independent (below the cross-over scale), hence degenerate with the bias. After bias marginalization, the best fit corresponds to the ΛCDM+GR model. However, for this particular model there are no published constraints in the literature, so our analysis presents a first result on that (studies on similar models can be found in Sahni & Shtanov 2003; Giannantonio, Song & Koyama 2008; Lombriser et al. 2009). Note that a cross-over scale of $r_c \sim 300$ Mpc implies strong modifications to gravity on larger scales, and the ISW effect in the CMB is likely to be able to constrain such values as well.

7 CONCLUSIONS

In this work, we showed that we can use RSD to test cosmological models, by measuring the monopole and quadrupole of the correlation function of galaxies, $\{\xi_0, \xi_2\}$. The methodology and robust measurement of the correlation function presented in Raccanelli et al. (2010) and Samushia et al. (2012), which includes a careful treatment of corrections due to the geometry of the system, allows us to use those multipoles in a wider range of scales with respect to most standard analyses, and so have better constraints on the models tested. As shown in Samushia et al. (2012), most of the approximations assumed in the Kaiser analysis need to be dropped to have precise measurements of the correlation function, and so of the growth rate, whose deviation from the ΛCDM+GR expected value would imply the need of a new cosmological model. For current analysis, the wide angle corrections are not important; their importance will depend on survey characteristics, and a detailed analysis of that is beyond the scope of this paper. In general, they should be taken into account when $\theta \gtrsim 0.1$ rad or, at high-z, when the separation scale is very large; in that case, though, also general relativistic corrections will be important (see e.g. Yoo 2010; Bonvin & Durrer 2011; Challinor & Lewis 2011; Bertacca et al. 2012; Jeong, Schmidt & Hirata 2012; Yoo et al. 2012).

We explored the UDM (Bertacca et al. 2008, 2010) and the normal branch DGP (Schmidt 2009) models, that present deviations from the ΛCDM+GR scenario. Both classes of models are parametrized by one additional number: the speed of sound c_∞ and the cross-over scale r_c for UDM and nDGP, respectively. The value of these parameters affects both the growth rate parameter γ and the wide-angle corrections. Moreover, UDM models are characterized by a growth rate parameter, γ, that depends on $\{k, z, c_\infty\}$. After deriving its analytic expression, we used it to compute the predicted moments of the correlation function.

We then compared observations of LRGs from SDSS-II DR7 with theoretical predictions from the two cosmologies. This analysis allowed us to tighten the constraints on the speed of sound of UDM

Table 1. Constraints and best fits for models considered, when knowledge of the bias is assumed and after marginalizing over it as a free parameter, for the $r_{max} = 80$ and $120\,h^{-1}$ Mpc cases.

Model	1σ	2σ	3σ	Best fit
UDM[80], fixed bias	$c_\infty \leq$ 2.1e-4	$c_\infty \leq$ 3.8e-4	$c_\infty \leq$ 4.7e-4	$c_\infty = 0$ (ΛCDM)
UDM[80], marginalized	$c_\infty \leq$ 5.8e-4	$c_\infty \leq$ 6.3e-4	$c_\infty \leq$ 6.9e-4	$c_\infty =$ 5.0e-4
UDM[120], fixed bias	$c_\infty \leq$ 1.9e-4	$c_\infty \leq$ 3.5e-4	$c_\infty \leq$ 4.3e-4	$c_\infty = 0$ (ΛCDM)4
UDM[120], marginalized	$c_\infty \leq$ 5.8e-4	$c_\infty \leq$ 6.1e-4	$c_\infty \leq$ 6.9e-4	$c_\infty =$ 5.0e-4
nDGP[80], fixed bias	$r_c \geq$ 12 580 (Mpc)	$r_c \geq$ 7040 (Mpc)	$r_c \geq$ 5500 (Mpc)	$r_c =$ 25 000 (Mpc)
nDGP[80], marginalized	$r_c \geq$ 660 (Mpc)	$r_c \geq$ 290 (Mpc)	$r_c \geq$ 255 (Mpc)	$r_c = \infty$ (ΛCDM)
nDGP[120], fixed bias	$r_c \geq$ 9803 (Mpc)	$r_c \geq$ 6480 (Mpc)	$r_c \geq$ 5050 (Mpc)	$r_c =$ 20 000 (Mpc)
nDGP[120], marginalized	$r_c \geq$ 1237 (Mpc)	$r_c \geq$ 340 (Mpc)	$r_c \geq$ 270 (Mpc)	$r_c = \infty$ (ΛCDM)

models to $c_\infty \leq 6.1 \times 10^{-4}$, and to put, for the first time, a lower bound on the cross-over scale for the nDGP model considered of 340 Mpc, both at 95 per cent confidence level. It is worth noting that the results would largely benefit from a better knowledge of the bias that could be obtained combining information from other cosmological probes, as e.g. gravitational lensing.

We showed the potential of this methodology for constraining alternative cosmological models, in particular when future surveys will provide access to a wider range of scales, hence allowing a tomographic analysis, which will be essential to break degeneracy between cosmological parameters.

ACKNOWLEDGEMENTS

Part of the research described in this paper was carried out at the Jet Propulsion Laboratory, California Institute of Technology, under a contract with the National Aeronautics and Space Administration. AR would like to thank for the hospitality the Institute of Cosmology and Gravitation at the University of Portsmouth, where part of this work was carried out. FS is supported by the Gordon and Betty Moore Foundation at Caltech. WJP is grateful for support from the European Research Council and STFC. LS acknowledges support from European Research Council, Georgian National Science Foundation grant ST08/4-442 and SNSF (SCOPES grant No. 128040).

REFERENCES

Abazajian K. N. et al., 2009, ApJS, 182, 543
Afshordi N., Geshnizjani G., Khoury J., 2009, J. Cosmol. Astropart. Phys., 08, 030
Bertacca D., Bartolo N., 2007, J. Cosmol. Astropart. Phys., 0711, 026
Bertacca D., Bartolo N., Diaferio A., Matarrese S., 2008, J. Cosmol. Astropart. Phys., 0810, 023
Bertacca D., Bartolo N., Matarrese S., 2010, Adv. Astron., 2010, 904379
Bertacca D., Raccanelli A., Piattella O., Pietrobon D., Bartolo N., Matarrese S., Giannantonio T., 2011, J. Cosmol. Astropart. Phys., 1103, 039
Bertacca D., Maartens R., Raccanelli A., Clarkson C., 2012, J. Cosmol. Astropart. Phys., 10, 025
Bharadwaj S., 1996, ApJ, 472, 1
Blake C. et al., 2011, MNRAS, 415, 2876
Bonvin C., Durrer R., 2011, Phys. Rev. D, 84, 063505
Brans C. H., 2005, preprint (arXiv:gr-qc/0506063)
Cabré A., Gaztañaga E., 2009, MNRAS, 393, 1183
Camera S., Bertacca D., Diaferio A., Bartolo N., Matarrese S., 2009, MNRAS, 399, 1995
Camera S., Kitching T. D., Heavens A. F., Bertacca D., Diaferio A., 2011, MNRAS, 415, 399
Camera S., Carbone C., Moscardini L., 2012, J. Cosmol. Astropart. Phys., 1203, 039
Carroll S. M., Duvvuri V., Trodden M., Turner M. S., 2004, Phys. Rev. D, 70, 043528
Challinor A., Lewis A., 2011, Phys. Rev. D, 84, 043516
Cole S., Fisher K. B., Weinberg D. H., 1995, MNRAS, 275, 515
Crocce M., Scoccimarro R., 2006, Phys. Rev. D, 73, 063519
Crocce M., Scoccimarro R., 2008, Phys. Rev. D, 77, 023533
Dalal N., Doré O., Huterer D., Shirokov A., 2008, Phys. Rev. D, 77, 123514
Deffayet C., 2001, Phys. Lett. B, 502, 199
de Rham C., Hofmann S., Khoury J., Tolley A. J., 2008, J. Cosmol. Astropart. Phys., 2, 11
Desjacques V., Seljak U., 2010, Classical Quantum Gravity, 27, 124011
Durrer R., Maartens R., 2008, Gen. Relativ. Gravit., 40, 301
Dvali G., Gabadadze G., Porrati M., 2000, Phys. Lett. B, 485, 208
Eisenstein D. J., Hu W., 1998, ApJ, 496, 605
Eisenstein D. J. et al., 2001, AJ, 122, 2267
Eisenstein D. J., Seo H.-J., White M., 2007, ApJ, 665, 14
Fukugita M., Ichikawa T., Gunn J. E., Doi M., Shimasaku K., Schneider D. P., 1996, AJ, 111, 1748
Giannantonio T., Song Y. S., Koyama K., 2008, Phys. Rev. D, 78, 044017
Gregory R., Kaloper N., Myers R. C., Padilla A., 2007, J. High Energy Phys., 10, 69
Gunn J. E. et al., 1998, AJ, 116, 3040
Guzzo L. et al., 2008, Nat, 451, 541
Hamilton A. J. S., 1992, ApJ, 385, L5
Hamilton A. J. S., 1998, in Hamilton D., ed., The Evolving Universe. Kluwer, Dordrecht, p. 185
Hawkins E. et al., 2003, MNRAS, 346, 78
Jackson J. C., 1972, MNRAS, 156, 1
Jain B., Zhang P., 2007, Phys. Rev. D, 78, 063503
Jeong D., Schmidt F., Hirata C. M., 2012, Phys. Rev. D, 85, 023504
Kaiser N., 1987, MNRAS, 227, 1
Kazin E. et al., 2010, ApJ, 710, 1444
Koyama K., Maartens R., 2006, J. Cosmol. Astropart. Phys., 1, 16
Kwan J., Lewis G. F., Linder E. V., 2012, ApJ, 748, 78
Landy S. D., Szalay A. S., 1993, ApJ, 412, 64
Linder E., 2005, Phys. Rev. D, 72, 043529
Linder E., 2007, Astropart. Phys., 29, 336
Lombriser L., Hu W., Fang W., Seljak U., 2009, Phys. Rev. D, 80, 063536
Luty M. A., Porrati M., Rattazzi R., 2003, J. High Energy Phys., 09, 029
Marulli F., Bianchi D., Branchini E., Guzzo L., Moscardini L., Angulo R. E., 2012, MNRAS, 426, 2566
Matarrese S., Pietroni M., 2007, J. Cosmol. Astropart. Phys., 0706, 026
Matarrese S., Verde L., 2008, ApJ, 677, L77
Matsubara T., 2004, ApJ, 615, 573
Matsubara T., 2008a, Phys. Rev. D, 77, 063530
Matsubara T., 2008b, Phys. Rev. D, 78, 083519
Nesseris S., Perivolaropoulos L., 2008, Phys. Rev. D, 77, 023504
Nicolis A., Rattazzi R., 2004, J. High Energy Phys., 6, 59
Okumura T., Matsubara T., Eisenstein D. J., Kayo I., Hikage C., Szalay A. S., Schneider D. P., 2008, ApJ, 676, 889
Papai P., Szapudi I., 2008, MNRAS, 389, 292
Peacock J. A., Dodds S. J., 1996, MNRAS, 280, L19
Peacock J. A. et al., 2001, Nat, 410, 169
Percival W. J., Schäfer B. M., 2008, MNRAS, 385, L78
Perlmutter S. et al., 1999, ApJ, 517, 565
Piattella O., Bertacca D., 2011, Modern Phys. Lett. A, 26, 2277
Pope A. C. et al., 2004, ApJ, 607, 655
Raccanelli A., Samushia L., Percival W. J., 2010, MNRAS, 409, 1525
Reid B. A., White M., 2011, MNRAS, 417, 1913
Reid B. A. et al., 2012, MNRAS, 426, 2719
Riess A. G. et al., 1998, AJ, 116, 1009
Ross A. et al., 2011, MNRAS, 417, 1350
Ross A. et al., 2012, MNRAS, 424, 564
Sahni V., Shtanov Y., 2003, J. Cosmol. Astropart. Phys., 0311, 014
Samushia L., Percival W. J., Raccanelli A., 2012, MNRAS, 420, 3
Sanchez A. G. et al., 2012, MNRAS, 425, 415
Schmidt F., 2009, Phys. Rev. D, 80, 12
Scoccimarro R., 2004, Phys. Rev. D, 70, 083007
Slosar A., Hirata C., Seljak U., Ho S., Padmanabhan N., 2008, J. Cosmol. Astropart. Phys., 08, 031
Song Y.-S., Koyama K., 2009, J. Cosmol. Astropart. Phys., 01, 048
Song Y.-S., Percival W. J., 2009, J. Cosmol. Astropart. Phys., 0910, 004
Szalay A. S., Matsubara T., Landy S. D., 1998, ApJ, 498, L1
Szapudi I., 2004, Phys. Rev. D, 70, 083536
Taruya A., Nishimichi T., Saito S., 2010, Phys. Rev. D, 82, 063522
Tegmark M. et al., 2006, Phys. Rev. D, 74, 123507
Thomas S. A., Abdalla F. B., Lahav O., 2011, Phys. Rev. Lett., 106, 241301
Varshalovich D. A., Moskalev A. N., Khershonski V. K., 1988, Quantum Theory of Angular Momentum. World Scientific Press, Singapore
Xia J.-Q., Bonaldi A., Baccigalupi C., De Zotti G., Matarrese S., Verde L., Viel M., 2010, J. Cosmol. Astropart. Phys., 1008, 013

Yamamoto K., Sato T., Hütsi G., 2008, Prog. Theor. Phys., 120, 609
Yamamoto K., Nakamura G., Hütsi G., Narikawa T., Sato T., 2010, Phys. Rev. D, 81, 103517
Yoo J., 2010, Phys. Rev. D, 82, 083508
Yoo J., Hamaus N., Seljak S., Zaldarriaga M., 2012, Phys. Rev. D, 86, 063514
Zaroubi S., Hoffman Y., 1993, ApJ, preprint (astro-ph/9311013)
Zehavi I. et al., 2005, ApJ, 621, 22

APPENDIX A: METHODOLOGY

A1 The wide-angle corrections

Most previous RSD analyses have used the simple plane-parallel approximation given by the Kaiser formula. In this case, a Fourier mode $\hat{\delta}^s(\boldsymbol{k})$ in redshift space is simply equal to the unredshifted mode $\hat{\delta}(\boldsymbol{k})$ amplified by a factor $1+\beta\mu_k^2$:

$$\hat{\delta}^s(\boldsymbol{k}) = \left(1+\beta\mu_k^2\right)\hat{\delta}(\boldsymbol{k}), \tag{A1}$$

where $\beta = f/b$, with b being the bias. This correction arises from the Jacobian of equation (2), when the $(1+\frac{v}{r})^2$ term is neglected.

The wide-angle linear redshift-space correlation function and power spectrum have been analytically derived by Zaroubi & Hoffman (1993), Szalay, Matsubara & Landy (1998), Szapudi (2004), Matsubara (2004), Papai & Szapudi (2008), and tested against both simulations (Raccanelli et al. 2010) and real data (Samushia et al. 2012).

Papai & Szapudi (2008) have argued that, for wide angles, the v/r term in equation (2) is of the same order as the $\partial_r v$ term. As a consequence, a careful and precise analysis of the correlation function, requires the full (linear) Jacobian, dropping the distant-observer approximation. In this case, we can express the linear overdensity as

$$\delta^s(s) = \int \frac{\mathrm{d}^3k}{(2\pi)^3}\mathrm{e}^{\mathrm{i}k_j\cdot r_j}\left[1+f(\hat{\boldsymbol{r}}_j\cdot\hat{\boldsymbol{k}}_j)^2 - \mathrm{i}\alpha(r)f\frac{\hat{\boldsymbol{r}}_j\cdot\hat{\boldsymbol{k}}_j}{rk}\right]\delta(k); \tag{A2}$$

the redshift-space correlation function reads

$$\begin{aligned}\xi^s &= \langle\delta^s(\boldsymbol{s}_1)\delta^{s*}(\boldsymbol{s}_2)\rangle = \int\frac{\mathrm{d}^3k}{(2\pi)^3}P(k)\mathrm{e}^{\mathrm{i}k(r_1-r_2)}\\ &\times\left[1+\frac{f}{3}+\frac{2f}{3}L_2(\hat{\boldsymbol{r}}_1\cdot\hat{\boldsymbol{k}}) - \frac{\mathrm{i}\alpha(r)f}{r_1k}L_1(\hat{\boldsymbol{r}}_1\cdot\hat{\boldsymbol{k}})\right]\\ &\times\left[1+\frac{f}{3}+\frac{2f}{3}L_2(\hat{\boldsymbol{r}}_2\cdot\hat{\boldsymbol{k}}) + \frac{\mathrm{i}\alpha(r)f}{r_2k}L_1(\hat{\boldsymbol{r}}_2\cdot\hat{\boldsymbol{k}})\right].\end{aligned} \tag{A3}$$

The third terms in the brackets describe the wide-angle effects, while the fourth ones are responsible for the so-called mode coupling. The r_1 and r_2 terms in the denominator depend on the angular separation of the galaxies, and α is proportional to the logarithmic derivatives of the galaxy distribution function (equation 3). We refer to Fig. A1 for the geometry of the problem, where we define 2θ to be the angular separation of the two galaxies considered, ϕ_1 as the angle between the vector to the first galaxy in a pair $\boldsymbol{r}_1$ and $\boldsymbol{r}$, $\boldsymbol{r}$ to be the vector connecting galaxies in a pair, and ϕ_2 to be the angle between vector to the second galaxy in a pair $\boldsymbol{r}_2$ and $\boldsymbol{r}$.

Tripolar spherical harmonics are the most natural basis for the expansion of a function that depends on three directions (Varshalovich, Moskalev & Khershonski 1988), so, as suggested by Szapudi (2004) and Papai & Szapudi (2008), we expand equation (A3) using a subset of them, so that the redshift-space correlation function can then be written as

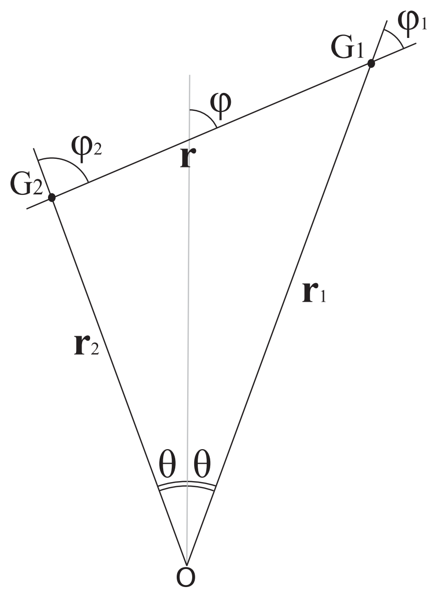

Figure A1. The coordinate system adopted for the triangle formed by the observer O, and galaxies G_1 and G_2.

$$\xi^s(\hat{r}_1,\hat{r}_2,\hat{r}) = \sum_{\ell_1,\ell_2,\ell} B^{\ell_1\ell_2\ell}(r,\phi_1,\phi_2)S_{\ell_1\ell_2\ell}(\hat{r}_1,\hat{r}_2,\hat{r}), \tag{A4}$$

where $B^{\ell_1\ell_2\ell}(r,\phi_1,\phi_2)$ are a series of coefficients that depend on f, $g_i(\phi_i)$ and $\xi_\ell^r(r)$ (see Raccanelli et al. 2010, for details on the definition of these functions). These coefficients can be divided into two different subsets: one that depends on the third term inside the brackets in equation (A3), given by $B^{\ell_1\ell_2\ell}(r)$, with $\ell_1\ell_2\ell$ combinations of 0, 2, 4, with only the radial dependence accounting for the wide-angle effects, and one that depends on the fourth terms inside the brackets of equation (A3), given by $B^{\ell_1\ell_2\ell}(r,\phi_1,\phi_2)$, with $\ell_1\ell_2\ell$ combinations of 0, 1, 2, 3, with also an angular dependence, describing the mode coupling part (see Szalay et al. 1998; Szapudi 2004; Papai & Szapudi 2008, for a detailed derivation). The plane-parallel approximation emerges as a limit when $\hat{r}_1 = \hat{r}_2$. This formalism was shown to accurately reproduce wide-angle effects seen in numerical simulations (Raccanelli et al. 2010).

A2 SDSS DR7

An extensive analysis of the SDSS DR7 data is provided in Samushia et al. (2012); we refer the reader to that paper for the full details on the analysis of SDSS DR7 data and for the relative importance of various corrections considered. In the following we use the measurements of moments of the correlation function presented there, to test models of gravity.

A2.1 Distribution of θ and μ

For surveys that cover a significant fraction of the sky, the distribution of galaxies pairs has a complicated dependence on the variables $\{r,\mu,\theta\}$, since not all sets of their combinations are equally likely or even geometrically possible. In particular, the distribution of μ does not correspond to that of an isotropic pair distribution, and this will strongly bias measurements of angular moments of the correlation

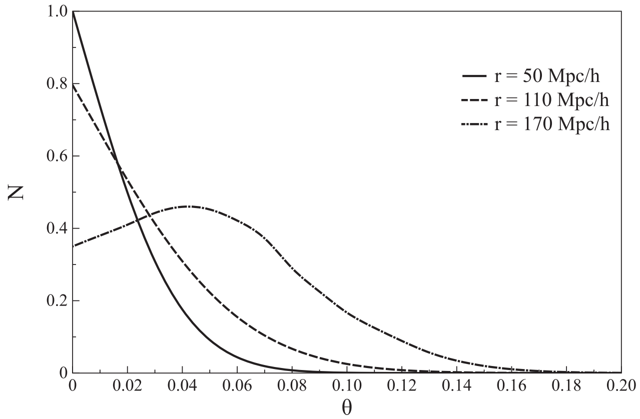

Figure A2. Measured distribution of angular separation θ for LRG pairs in the SDSS DR7 catalogue, at different scales.

function. We can see in this appendix the effects on the correlation function of a non-zero fixed angular separation, and in Section 4.1 that these errors can bias our estimate of the γ parameter.

In Fig. A2 is shown the distribution of θ of observed LRGs in the SDSS DR7 catalogue. As expected, in this case the number of pairs with relatively large θ is very small, and it increases with the linear separation of pairs.

Other than the wide angle and the mode coupling corrections, there is also another difference that has to be taken in account when doing a real-data wide-angle analysis, that derives from the fact that the distribution of galaxies in μ will be non-trivial, with some values of μ not permitted for non-zero θ. As a consequence, we will not be able to measure pure Legendre moments of the correlation function, but instead we will need to use weighted integrals and biased moments; corrections due to a non-uniform 'μ-distribution' can be applied to both plane-parallel and wide-angle analyses. In Fig. A3 is shown the distribution of μ for observed LRGs in the SDSS DR7 catalogue.

A2.2 Non-linear effects

We model two non-linear effects: one due to the baryonic acoustic oscillations (BAO) peak and the other due to the so-called Fingers-of-God (FOG). Since we are only interested in the signal on large scales, where the linear theory is an accurate description, we assume that the non-linear effects are small, except for the fact that the matter power spectrum itself goes non-linear. We describe the non-linear contribution of the power spectrum by means of a two-component model, which splits $P(k)$ into a 'smooth' part that describes the overall shape and a 'wiggled' part, which describes the BAO:

$$P_{\rm BAO}(k,\mu) = P_{\rm full}(k,\mu) - P_{\rm smooth}(k,\mu). \quad \text{(A5)}$$

The primary non-linear effect on the BAO component of the power spectrum is a damping on small scales, which can be well approximated by a Gaussian smoothing (Bharadwaj 1996; Crocce & Scoccimarro 2006, 2008; Eisenstein, Seo & White 2007; Matarrese & Pietroni 2007; Matsubara 2008a,b):

$$P^{\rm nl}_{\rm BAO}(k,\mu) = P^{\rm lin}_{\rm BAO}(k,\mu)\exp\left\{-k^2\left[\frac{(1-\mu^2)\Sigma_\perp}{2}+\frac{\mu^2\Sigma_{||}}{2}\right]\right\}, \quad \text{(A6)}$$

where $\Sigma_\perp = \Sigma_0 D$ and $\Sigma_{||} = \Sigma_0(1+f)D$; Σ_0 is a constant phenomenologically describing the diffusion of the BAO peak due to non-linear evolution. From *N*-body simulations its numerical value is of order $10\,h^{-1}$ Mpc and seems to depend linearly on σ_8 but only weakly on k and other cosmological parameters.

Within dark matter haloes the peculiar velocities of galaxies are highly non-linear. These velocities can induce RSD that are larger than the real-space distance between galaxies within the halo. This gives rise to the observed FOG effect, that is a strong elongation of structures along the line of sight (Jackson 1972). The FOG effect sharply reduces the power spectrum on small scales compared to the predictions of the linear model, and is usually modelled by multiplying the linear power spectrum by a function F that depends on the average velocity dispersion of galaxies within the relevant haloes, σ_v, k and μ. The most common one is a Gaussian damping (see e.g. Cole, Fisher & Weinberg 1995; Peacock & Dodds 1996):

$$F(\sigma_v,k,\mu) = \exp\left[-(k\sigma_v\mu)^2\right] \quad \text{(A7)}$$

that is small on small scales and approaches unity for scales larger than $1/\sigma_v$.

A3 The estimator of the correlation function moments

To estimate the moments of the correlation function we use Landy–Szalay-type estimators (Landy & Szalay 1993):

$$\hat{\xi}_\ell(r_i) = L_\ell(\mu) \times \frac{\sum_{j,k}\left[DD(r_i,\mu_j,\theta_k) - 2DR(r_i,\mu_j,\theta_k) + RR(r_i,\mu_j,\theta_k)\right]}{\sum_{j,k}\left[RR(r_i,\mu_j,\theta_k)\right]}, \quad \text{(A8)}$$

where $\mu = \cos(\varphi)$, while $DD(r_i,\mu_j,\theta_k)$, $DR(r_i,\mu_j,\theta_k)$ and $RR(r_i,\mu_j,\theta_k)$ are the number of galaxy–galaxy, galaxy–random and random–random pairs in bins centred on r_i, μ_j and θ_k.

RSD measurements are often extracted from the normalized quadrupole Q (Hamilton 1992), defined as

$$Q(r) = \frac{\xi_2(r)}{\xi_0(r) - \frac{3}{r^3}\int_0^r \xi_0(r')r'^2{\rm d}r'}. \quad \text{(A9)}$$

The normalized quadrupole Q was introduced because it is independent of the shape of the power spectrum, and so it depends only on the β parameters, allowing to directly test gravity; however, this is true only in the Kaiser analysis, and so it is not true in our case. For this reason we test different cosmological models fitting the moments of the correlation function, ξ_0, ξ_2.

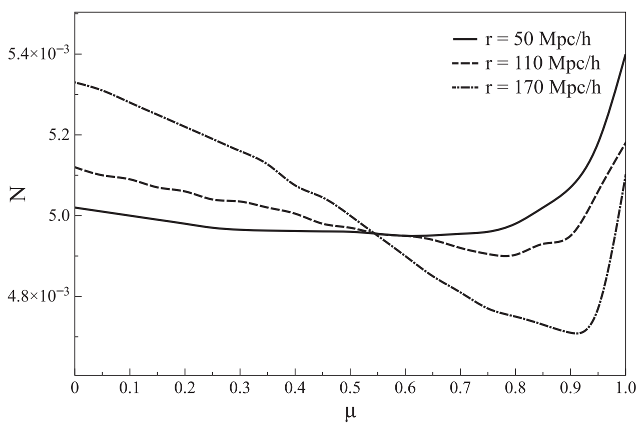

Figure A3. Measured distribution of orientation angle μ for LRG pairs in the SDSS DR7 catalogue, at different scales.

We compute error bars as the square root of the diagonal terms in the covariance matrix:

$$\mathbf{C} = \frac{1}{79} \sum \left[\hat{\boldsymbol{X}}(r_i) - \overline{X}(r_i)\right] \left[\hat{\boldsymbol{X}}(r_j) - \overline{X}(r_j)\right], \tag{A10}$$

where $\hat{\boldsymbol{X}}(r)$ is a vector of the measurements of ξ_0, ξ_2 at scale r and $\overline{X}$ is the mean value from all 80 mock catalogues.

We compare measurements with predictions from different models, where we compute the redshift-space correlation function including effects from wide angle and μ-distribution as well as survey geometry and non-linearities. Estimates of Legendre moments given by equation (A8) correspond to

$$\tilde{\xi}_\ell(r) = \int W_r(r, \theta, \mu)\, \xi^s(r, \theta, \mu)\, L_\ell(\mu)\, \mathrm{d}\theta\, \mathrm{d}\mu, \tag{A11}$$

where $W_r(r, \theta, \mu)$ is a weight function that appears because of the geometrical constraints and the not uniform distribution of μ, as explained in Section A1 and gives the relative number of pairs in a survey that form angles μ and θ for a given scale r; when the θ distribution tends towards a delta function centred at $\theta = 0$, the wide-angle effects become negligible, while when the distribution in μ tends towards a uniform one, this effect becomes negligible. The correlation function of equation (A4) can be written as

$$\xi^s(r, \theta, \varphi) = \sum_{ab} c_{ab}(f, r) L_a[\cos(\theta)] L_b[\cos(\varphi)], \tag{A12}$$

where $\{r, \theta, \varphi\}$ are as in Fig. A1, and $c_{ab}(f, r)$ are coefficients that depend on the separation between galaxies and the f of equation (6) (see Szapudi 2004; Papai & Szapudi 2008; Raccanelli et al. 2010 for further details).

A4 LasDamas mocks

In this paragraph we show our measurements from the LasDamas simulations and the ΛCDM+GR model prediction. As one can see in Figs A4 and A5, the LasDamas set reproduces quite well the measured moments of the correlation function, the main deviation being on large scales of the monopole of the correlation function, that represents also the main source of deviation from ΛCDM+GR at the scales we considered; however, the other models do not help much in picking up that deviation. This is a well-known discrepancy between theoretical predictions and observations, and it has been detected in spectroscopic (Kazin et al. 2010; Samushia et al. 2012) and photometric (Thomas, Abdalla & Lahav 2011) data sets. This excess power at large scale can be induced by primordial non-Gaussianity (see e.g. Dalal et al. 2008; Matarrese & Verde 2008; Slosar et al. 2008; Desjacques & Seljak 2010; Xia et al. 2010) or exotic physics (Thomas et al. 2011); however, Samushia et al. (2012) found that the redshift dependence of the excess power is different from what would be caused by non-Gaussianity, and Ross et al. (2011) suggest that this is likely to be due to masking effects from stellar sources. After correcting for systematics, Ross et al. (2012) found consistency at better than 2σ between the BOSS CMASS DR9 large-scale clustering data and the *WMAP* LCDM cosmological model. Further tests using mocks suggested that there was no evidence that additional potential systematic trends contributed individually at a level above that expected through noise. But, there is always the potential for more systematic problems to be present, or for the combination (which always tends to add power) not to have a more significant contribution – i.e. form part of the 2σ discrepancy.

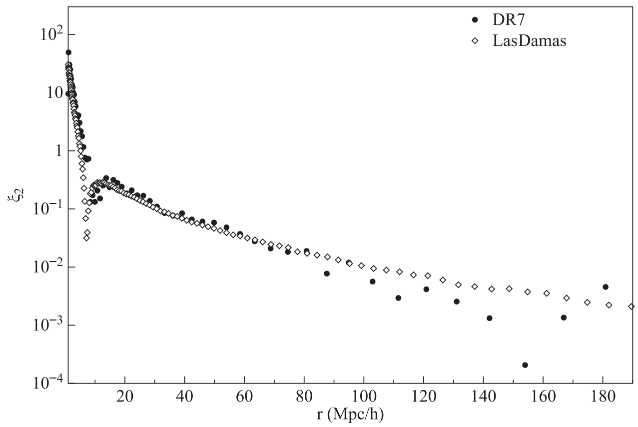

Figure A5. ξ_2 measured from 80 LasDamas mock catalogues and from SDSS DR7 data.

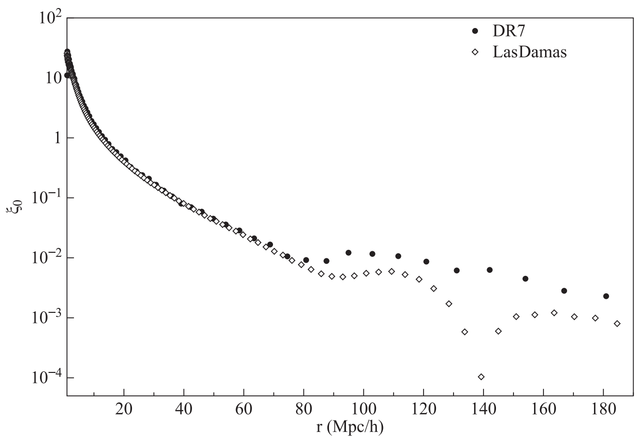

Figure A4. ξ_0 measured from 80 LasDamas mock catalogues and from SDSS DR7 data.

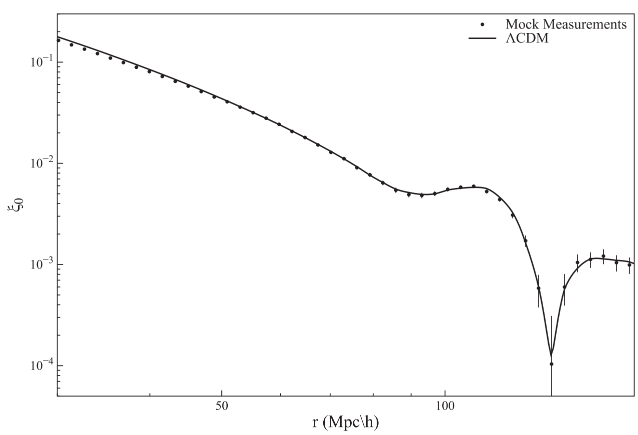

Figure A6. ξ_0 measured from 80 LasDamas mock catalogues and theoretical predictions for ΛCDM+GR.

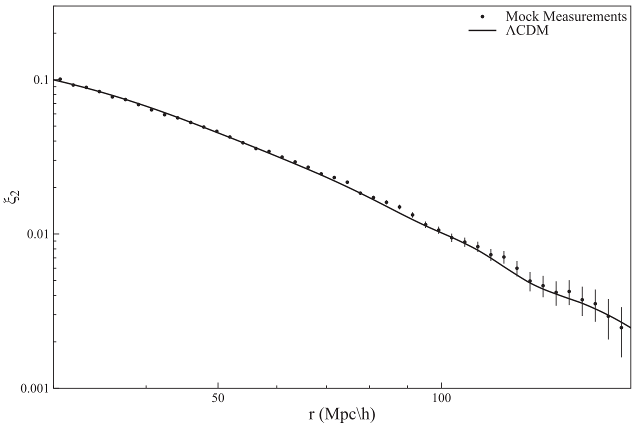

Figure A7. ξ_2 measured from 80 LasDamas mock catalogues and theoretical predictions for ΛCDM+GR.

Figs A6 and A7 show that our methodology, that includes corrections due to non-linearities, wide angle and μ-distributions, can fit the ΛCDM+GR simulations very well, up to scales of $180\,h^{-1}$ Mpc. For the data analyses, however, we decided to use as a maximum scale $r = 120\,h^{-1}$ Mpc.

This paper has been typeset from a TEX/LATEX file prepared by the author.